

Magnetic conjugate point observations of kilometer and hundred meter-scale irregularities and zonal drifts

E.R. de Paula¹, M.T.A.H. Muella¹, J.H.A. Sobral¹, M.A. Abdu¹, I.S. Batista¹, T.L. Beach²,
K.M. Groves²

¹*Divisão de Aeronomia, Instituto Nacional de Pesquisas Espaciais, São José dos Campos, 12227-010, SP, Brazil*

²*Space Vehicles Directorate, Air Force Research Laboratory, Hanscom AFB, MA 01731, USA*

Abstract

The Conjugate Point Equatorial Experiment (COPEX) campaign was carried out in Brazil, between October and December 2002, to study the conjugate nature of plasma bubble irregularities and to investigate their generation mechanisms, development characteristics, spatial-temporal distribution and dynamics. In this work we will focus mainly in the zonal spaced GPS (1.575 GHz) and VHF (250 MHz) receivers' data collected simultaneously at two magnetic conjugate sites of the COPEX geometry: Boa Vista and Campo Grande. These GPS/VHF receivers were set up to detect the equatorial scintillations and to measure ionospheric scintillation pattern velocities. Then, the zonal irregularity drift velocities were estimated by applying a methodology that corrects the effects due to vertical drifts and geometrical factors. The results reveal the coexistence of kilometer (VHF) and hundred-meter scale (GPS L-band) irregularities into the underlying depletion structure. Over the conjugate site of Campo Grande, the average zonal velocity at VHF

seems to be consistently larger than the estimated GPS velocities until about 02:00 UT, whereas over Boa Vista the irregularities detected from both techniques are drifting with comparable velocities. The hundred meter scale structures causing L-band scintillations appear to be drifting with comparable velocities over both the conjugate sites, whereas the kilometer scale structures are drifting over Campo Grande with larger average velocities (before 03:00 UT). Complementary data of ionospheric parameters scaled from collocated digital ionosondes are used in the analysis to explain differences/similarities on the scintillation/zonal drift results.

1. Introduction

Equatorial ionospheric spread F /plasma bubble (ESF/EPB) irregularities and their zonal drift velocities have been extensively studied in the past several decades by means of different experimental techniques. Depending upon the observational technique and the radio frequency used to monitor the ionosphere, the variability, structure and dynamics of the irregularities with different scale sizes can be probed by different instruments. As for the most recent technologies of the Global Navigation Satellite System (GNSS) applications, such as the Global Positioning System (GPS), single and spaced antenna systems have been used to monitor, respectively, the activity and dynamics of the irregularities that cause fluctuations/scintillations into the L-band signals [*Pi et al.*, 1997; *Beach and Kintner*, 1999; *Kil et al.*, 2000; *de Paula et al.*, 2002, 2007; *Ledvina et al.*, 2004; *Kintner et al.*, 2004; *Muella et al.*, 2009].

It is well known that the rapid increase of the eastward electric fields during the post-sunset hours (and the bottomside instabilities generated by Rayleigh-Taylor plasma

mechanism) is the main prerequisite (and source) responsible for the generation (triggering) of ESF/EPB irregularities. According to *Haerendel* [1973], the primary instabilities can be followed by others secondary plasma instabilities which can lead to a cascading process, and give origin to a wide spectrum of irregularity structures with different scale sizes and characteristics. *Basu et al.* [1978] have shown, based on multifrequency observations that irregularities with scale sizes varying from several meters to about 1 km may coexist during the generation/growth phase of EPB irregularities. Depending on the apex height reached above the magnetic equator, the large depleted density bubbles can extend/expand along the magnetic field lines to *F*-region heights over latitudes off the equator. Then, the extremities ‘feet’ of the bubbles intersect the crests of the equatorial ionization anomaly (EIA) at off-equatorial latitudes, a region of increased background electron density and sharp density gradients [*Muella et al.*, 2008b, 2010]. The presence of these gradients give rise, inside the bubbles, to conditions favorable for the generation of irregularities with different scale sizes [*Rao et al.*, 2006]. According to *Muralikrishna* [2000], small scale irregularities associated with large scale depletions can be generated in a region of downward electron density gradients since the ambient electric field is also downward. Therefore, the cross-field instability is possibly a causative secondary mechanism for the generation of small scale plasma irregularities.

It is known that EPBs are large scale plasma depleted regions aligned along the magnetic flux tubes which may extend beyond the poleward edge of the equatorial anomaly to dip latitudes ranging up 20° from the magnetic equator [*Sahai et al.*, 1981]. This feature allows the investigation from coordinated observations at conjugate sites of important aspects of the equatorial plasma bubbles, such as, their development characteristics and connections with sporadic *E*-layers, symmetry/asymmetry conditions, the role of the

evening vertical drift (transequatorial/meridional wind) in their development (suppression), day-to-day variability, latitudinal/temporal dependence of their zonal drift velocity, etc. For a better understanding of many of these aspects, the Conjugate Point Equatorial Experiment (COPEX) campaign of approximately 70-days duration was conceived and carried out at four observation sites in Brazil during October-December 2002. The COPEX campaign concerted efforts of many scientific groups (e.g. National Institute for Space Research/INPE - Brazil, Air Force Research Laboratory – USA, University of Massachusetts Lowell, Brazilian Air Force, and others) and the data collected during the observation period have also been used to validate the Communication/Navigation Outage Forecasting System (C/NOFS) satellite [*de La Beaujardière et al.*, 2004] prior to its launching in April 2008. The scientific objectives of the COPEX campaign and other relevant results published elsewhere using different instruments and techniques can be found in *Abdu et al.* [2009], *McDougall et al.* [2009], *Sobral et al.* [2009], *Batista et al.* [2008], *McNamara et al.* [2008], *Muella et al.* [2008b] and *Reinisch et al.* [2004].

In this paper, we present for the first time COPEX observations of simultaneous VHF (250 MHz) and GPS L-band (1.575 GHz) scintillations, which are sensitive to irregularities with different scale sizes (VHF is sensitive to ~1 km and GPS L1 frequency is sensitive to ~360-400 m for an irregularity layer at 350 km). The scintillations are known to be caused by irregularities embedded in the large-scale plasma bubble structures, and their eastward drift can be derived from ground-based GPS/VHF systems. Figure 1 shows the COPEX location and geometry on the central Brazilian territory. The configuration of the COPEX sites provides a unique opportunity to study the conjugate nature of the irregularities and the temporal/latitudinal dependence of their zonal drift velocities in a region of large magnetic declination. From the four COPEX sites two of them were located

at conjugate points, Boa Vista (2.8° N; 60.7° W; dip angle 22.05° N) and Campo Grande (20.5° S; 54.7° W; dip angle 22.32° S), and two near the magnetic equator, Cachimbo (9.5° S; 54.8° W; dip angle 4.25° S) and Alta Floresta (9.7° S; 56.0° W; dip angle 3.38° S) (not shown in Figure 1). The observations that we present here are intended to provide contributions to a better understanding of certain aspects of low-latitude ionospheric dynamics at conjugate points, such as, evolution and characteristics of different irregularity scale sizes, their variability, temporal and latitudinal dependence. The main objectives of this paper are to present a comparative study of scintillations and zonal drifts observed at GPS L1 and VHF frequencies, and to explain differences/similarities on the basis of ionospheric and irregularity characteristics. Complementary ionospheric data from collocated digital ionosondes are used in the present study.

The remaining sections of this work are as follows: section 2 presents the instrumentation and methodology to measure the scintillations and to estimate the irregularity drifts. Section 3 presents the results and discussions on the scintillation and zonal drift velocities monitored by ground-based GPS and VHF receivers. Section 4 presents the remarks and conclusions.

2. Experimental Techniques

2.1 VHF Spaced Antenna System

The VHF system used during the COPEX campaign was developed to monitor scintillations in the frequency range of 240-260 MHz from radio beacon signals received from geostationary satellites FLEETSAT-7 (longitude 100° W) and FLEETSAT-8 (longitude 23° W). Each VHF system consists of RF and IF converters, one dedicated

computer and a multiplex module for data processing and a set of four Yagi antennas. The antennas are installed in a magnetically spaced configuration, being two in the east direction and two in the west direction. A pair of antennas (CH#1-2) is separated by a distance of 100 m in the magnetic east-west direction and set up to detect signals from satellite FLEETSAT-7 (westerly link). The other pair (CH#3-4) of antennas with the same separation detects signals from satellite FLEETSAT-8 (easterly link). The characteristics of the signal paths from the two geostationary satellites are summarized in Table 1. It is noted that the signal ray path of the westerly link has lower elevation angle than that of the easterly link. For this reason we will analyze in this study only the scintillations measured from easterly link FLEETSAT-8 satellite whose elevation angle is above 46° in all COPEX sites, which reduces the effects of multipath and tropospheric scattering on the scintillation measurements. The equatorial site of the VHF receiver was located at Alta Floresta, which is separated by a distance of only ~ 130 km from Cachimbo.

The signal power data samples (100 Hz) recorded by the VHF data acquisition system are digitalized and used to compute accurate values of S_4 scintillation index for every 81.92 seconds. The S_4 index is the mostly used parameter to study amplitude scintillations due to radio wave diffractions caused by Fresnel scale irregularities embedded in background plasma of large density, and is defined as the normalized standard deviation of the received signal power intensity. From the S_4 records we show in this report the scintillation activity over all the COPEX sites throughout the campaign period. Then, for the nights with simultaneous VHF and GPS scintillation data, the morphology of the irregularities is discussed in terms of their intensity, onset time and time duration.

Zonal drift velocities for the nights with simultaneous scintillation records over the three conjugate sites are also estimated every 81.92 sec using the scintillation-based

spaced-antenna technique. Assuming frozen-in irregularity structures, the zonal scintillation pattern velocity is calculated from the time lag of the maximum cross-correlation of the scintillation pattern detected on the ground by the two spaced antenna (easterly link). However, it is known that depending on the orientation of the signal path and the localization of the ground receiver, this scintillation pattern velocity (V_{scint}) may have contributions of the vertical drift of the irregularities and, consequently, may be biased in relation to the zonal irregularity velocity at the ionospheric puncturing point (IPP) (*Ledvina et al.*, 2004), where:

$$V_{scint} = V_{ion} - V_Z \left[\frac{\tan(\phi)\sin(\theta)}{1 - \tan(\psi_{dip})\tan(\phi)\cos(\theta)} \right], \quad (1)$$

here V_{ion} is the zonal irregularity drift (positive eastward), V_Z is the contribution due to the vertical drift of the irregularities (positive upward), ψ_{dip} is the magnetic dip angle at the origin of the receiver coordinate system, ϕ is the satellite zenith angle and θ is the azimuth angle of the signal path obtained in the receiver coordinate system and measured clockwise with respect to the magnetic north. The contribution of the drift in the meridional direction can be assumed as negligible due to the extended nature of the irregularities along the magnetic field line [*Kintner et al.*, 2004]. Thus, for each COPEX site we estimate the zonal irregularity drift velocities (V_{ion}) from the scintillation pattern velocity (V_{scint}) by applying the cross-correlation technique and Eq. 1. In order to improve validity of the assumptions in the drift estimations we employ a cross-correlation threshold (c_i) ≥ 0.9 and a scintillation level threshold of (S_4) ≥ 0.25 . The 0.25 threshold for the S_4 index calculated from the VHF

measurements can be considered to be above the level of noise and multipath effects. Thus, by considering high threshold limit of 0.9 for peak cross-correlation and well-developed 250 MHz scintillations (i.e. $S_4 > 0.25$) we can assure that the corrections to the estimated scintillation pattern velocity (V_{scint}) required to yield the “true velocity” can be considered in our study negligible (Robert Livingston, personal communication). Moreover, as the focus of the present study is not concentrating on small differences in velocity at plasma bubble onset or other short periods of non-stationary scintillation time series, the time lag separation method in estimating V_{scint} can be considered appropriate.

However, to correct the contribution of the vertical irregularity drift an approximation is made by computing the time derivative of the F -region base height [$V_Z = d(h'F)/dt$] at 4 MHz return signal (close to the true height) scaled from the ionograms recorded at 10-min intervals. The contribution of V_Z is expected to be significant during the growth phase of the irregularities in the early evening owing to the electrodynamic $\mathbf{E} \times \mathbf{B}$ drift, however, the present method may underestimate the vertical plasma drift due to the effects of plasma recombination (for low F -layer heights (< 300 km)) and meridional winds (depending on their orientation). The signal path from the geostationary satellite FLEETSAT-8 to the VHF receivers is puncturing the ionosphere, at 350 km, in a sector of the sky that is spanning horizontally from ~ 303 - 312 km east of the overhead ionosphere seen by the digital ionosondes at the conjugate stations. We assume that the ambient ionospheric conditions in estimating V_Z do not change substantially over this distance. There should be around 10-11 min delay in the onset of ESF/EPB over Boa Vista and Campo Grande (as seen by the ionosondes) compared to that along the signal path to the VHF receivers. The subionospheric coordinates of the signal paths from the geostationary satellite FLEETSAT-8 intersecting the ionosphere at 350 km altitude, to the VHF receivers

at Boa Vista and Campo Grande, are shown in Table 2. The 350 km ionospheric points of FLEETSAT-8 map up along the field line to a height of ~620 km above the magnetic equator. Thus, scintillations observed at the conjugate sites of Boa Vista and Campo Grande correspond to equatorial bubbles at or above this altitude over the equatorial stations of Cachimbo/Alta Floresta. For this reason the subionospheric coordinates of the signal received at Alta Floresta is calculated for an ionospheric intersection point at 620 km. This corresponds to an horizontal distance of ~332 km and an approximately 12 min delay in the onset of ESF/EPB overhead Cachimbo compared to that along the signal path to Alta Floresta.

2.2 GPS Scintillation Monitoring System

During the COPEX campaign, two ground-based GPS receivers specially modified (SCINTillation MONitor-SCINTMON) to detect scintillations at L1 frequency (1.575 GHz) were installed (at each COPEX site) in a magnetically spaced configuration, and separated by a distance of 100 m along an east-west baseline. The SCINTMON receivers are based on GEC Plessey development system and consist of a 16-bit PC card making signal strength data recordings at every 20 ms. For each 1-min interval (3000 data samples) the signal power amplitude data are averaged and the S_4 scintillation index is computed using post-processing software [for more details see *Beach and Kintner, 2001*].

As mentioned before, for the nights with simultaneous GPS and VHF scintillation data over the COPEX sites, the morphology of the irregularities is studied in terms of their intensity, onset time and time duration. For comparison with the VHF scintillations we used in the analysis data from GPS satellites with elevation angle higher than 40°.

To estimate the mean zonal irregularity drift velocities (V_{ion}) using GPS scintillation-based spaced receiver measurements we used the following relation [Ledvina et al., 2004; Kintner and Ledvina, 2005]:

$$V_{scint} = \frac{h_{sat}}{h_{sat} - h_{ion}} \left\{ V_{ion} + (q_z/q_x) V_Z - \frac{h_{ion}}{h_{sat}} [V_{satx} + (q_y/q_x) V_{saty} + (q_z/q_x) V_{satz}] \right\}, \quad (2)$$

where V_{scint} is the zonal velocity in the receiver coordinated frame calculated by measuring the time lag of the maximum cross correlation of the amplitude scintillation patterns between the two-spaced receivers, h_{sat} and h_{ion} denote, respectively, the satellite height above the receivers' horizontal plane and the mean scattering height of the diffraction-causing irregularities, V_Z is the vertical irregularity velocity, v_{satx} , v_{saty} and v_{satz} are the zonal, meridional and vertical components of the satellite velocity, respectively, and (q_y/q_x) and (q_z/q_x) are the mapping factors of the scintillation pattern (and its velocity) that rotate all vectors into the local magnetic frame. The mapping factors are defined as [Ledvina et al., 2004]:

$$\frac{q_y}{q_x} = \frac{B_z/B_y \tan(\phi) \sin(\theta) - B_x/B_y}{1 - B_z/B_y \tan(\phi) \cos(\theta)}, \quad (3)$$

$$\frac{q_z}{q_x} = \frac{-\tan(\phi) \sin(\theta) + B_x/B_y \tan(\phi) \cos(\theta)}{1 - B_z/B_y \tan(\phi) \cos(\theta)}, \quad (4)$$

where B_z/B_y and B_x/B_y are ratios of the components of the magnetic field vectors at the ionospheric puncture point, ϕ is the satellite zenith angle and θ is the satellite azimuth

angle. In Eq. (2) V_{scint} and V_Z are obtained as in Eq. (1), h_{sat} and \vec{V}_{sat} are determined from satellite transmitted ephemerides, h_{ion} is considered as 350 km over the conjugate stations of Boa Vista and Campo Grande (as obtained from the mean values of $hmF2$), and the components of the magnetic field vector in the mapping factors q_y/q_x and q_z/q_x are determined at altitude h_{ion} from International Geomagnetic Reference Field (IGRF) model. It is noted from Eq. (2) that differently from Eq. (1) for VHF the zonal drift estimates are height sensitive.

Equation (2) is an extension of the method used by *Kil et al.* [2000], *de Paula et al.* [2002] and *Muella et al.* [2008b] for a more precise estimation of the zonal irregularity drift velocities by including geometrical effects. *Muella et al.* [2009] used Eq. (2) to estimate de zonal drifts at the equatorial station of São Luís (2.33° S, 44.21° W, dip latitude 1.3° S). However, in their estimations the vertical irregularity velocity could be neglected due to the numerous scintillating satellites signals used to average the scintillation pattern velocity over a period of several days and times [e.g. *Kintner and Ledvina*, 2005]. Averaging tends to reduce for quite small values the term $\tan(\phi)$ in the mapping factors (q_y/q_x) and (q_z/q_x), which in turn minimizes the effects of the vertical irregularity velocity in Eq. (2) [*Ledvina et al.*, 2004]. This approximation could also be used in the present study, but only those satellites whose signals are puncturing the ionosphere in the east sector of the sky (azimuth angle varying between 0° and 180°) above the stations were used in the zonal drift estimations. Since we limited our measurements to the easterly scintillating GPS signals, the number of satellites available reduces and, however, it seems appropriated to account in the estimations the contributions due to V_Z . From previous observations [*Kil et al.*, 2000; *Kintner et al.*, 2004] it has been noted for the GPS L1 signal that the contributions in V_{scint}

due to the random changes in the scintillation pattern is small (4% or less) and, thus we can approximate the mean apparent velocities (V_{scint}) to the true velocities. In the case of GPS derived zonal drifts we employ a cross-correlation threshold ($c_i \geq 0.9$) and a scintillation level threshold of ($S_4 \geq 0.2$). In addition, with the threshold limit of 0.9 for the peak cross-correlation, apparent and true velocities do not differ significantly and can be considered approximately the same. The zonal irregularity drift velocities estimated from the GPS scintillation measurements are then compared with those inferred from the VHF scintillation data at both conjugate sites.

3. Results and Discussions

3.1 Simultaneous VHF and GPS L1 Scintillation Activity

The contour plots in the panels from Figs. 2 and 3 depict the amplitude scintillation activity as detected, respectively, by the GPS and VHF receivers installed at the COPEX observation stations. The results for each station are presented in three panels, each panel representing the daily observations available during the months throughout the campaign period. The time scale in universal time (UT) refer to nocturnal period, where $UT = LT + 4h$. The color scale bars indicate the S_4 index levels used in the contour plots and the contours within the dashed lines indicate inexistence of data. For the GPS the contours in Fig. 2 represent the maximum scintillation index S_4 calculated for a GPS satellite with elevation angle $> 40^\circ$. It can be observed from this figure that the scintillation intensity is lower at the equatorial station of Cachimbo and tends to increase towards the conjugate sites of Boa Vista and Campo Grande. The lower scintillation levels over the dip equatorial station do not necessarily mean that the plasma bubble depletions are absent or weaker at

the dip equator than at off equatorial latitudes, but lie in the fact that for the GPS L-band frequencies the strong scintillations to occur require a significant background electron density [Makela, 2006]. In other words, the strength of the scintillations depends essentially on the integrated electron density deviation (ΔN), which is obtained from the product of the irregularity amplitude ($\Delta N/N$) and the background plasma density (N). The amplitude of the irregularity may be the same along the magnetic field lines but the background electron density varies with latitude. Thus, high scintillation levels could be expected to occur more frequently at off-equatorial latitudes in the region of the crests of the equatorial ionization anomaly (EIA). However, results from *Muella et al.* [2010] suggest that at latitudes of the EIA the most intense scintillations do not occur exactly at the crests, where the electron density is larger, but is more prone to be observed where sharp electron density gradients exist, that are, at the inner/outer edges of the enhanced anomaly crests.

Figure 2 also shows that, except in the last campaign days during December, the GPS scintillation activity at the conjugate station of Campo Grande is somewhat more intense than over Boa Vista. Considering the elongated nature of the plasma bubble structures along the geomagnetic field lines, one should expect a strong correspondence among the scintillations observed at both conjugate sites. However, Fig. 2 reveals asymmetrical features in the intensity and latitudinal distribution of the scintillations. It is known that large north-south asymmetry of the EIA, during the generation stage of the irregularities, reduces the instability growth rate through its control on the F -layer bottomside upward density gradients and the magnetic flux tube integrated conductivities [Maruyama, 1988; Abdu, 1997]. Otherwise, when the asymmetries in the ambient ionization at latitudes adjacent to the regions of the EIA arise during the developed phase of

the irregularities, this could be a possible cause for a corresponding asymmetry in the scintillation activity at magnetic conjugate points. Asymmetries in the electron density distribution in the regions of the EIA can be attributed to the action of transequatorial meridional neutral winds. Thus, the role of horizontal neutral winds is to modify the plasma surrounding the crests of the anomaly and also to affect the location, width and magnitude of the plasma density gradients. Since the occurrence of equatorial scintillations tends to be mostly confined within the boundaries of the anomaly, asymmetries in the ambient ionization and in the electron density gradients at latitudes adjacent to the regions of the EIA could be a possible cause for the corresponding scintillation asymmetries at the conjugate sites of Boa Vista and Campo Grande. More recently, *Abdu et al.* [2009] attributed to such asymmetries of ionization and gradients over conjugate sites, as the possible causes for the corresponding asymmetries observed in the echo intensities of digital ionosonde data. The magnetic conjugate stations of Boa Vista and Campo Grande are not expected to be located exactly under the crests of the EIA, but under the equatorward edge of the anomaly peaks.

Despite of the lack of data during some days, it may be noted from the simultaneous VHF scintillation data (S_4 index) in Fig. 3 that, over Campo Grande, the VHF scintillation activity is also somewhat more intense than over Boa Vista. Figure 3 shows that the VHF scintillations in the conjugate stations do not differ significantly from each other in terms of intensity until about 03:00 UT. However, it seems that over Campo Grande the scintillations tend to cease later and remain until about 06:00 UT on some days, whereas over Boa Vista the scintillations are more concentrated in the pre-midnight hours (until 04:00 UT). Figure 3 also shows that until around 01:00 UT the magnitude of the S_4 index observed at the equatorial station of Alta Floresta does not differ significantly from that

observed at the magnetic conjugate stations. The parameter $foF2$ scaled from ionograms recorded during the COPEX campaign can be used to evaluate the presence of asymmetries in the electron density distribution at the conjugate sites ($foF2$ is proportional to the square root of $NmF2$) and how it could be related with the scintillation asymmetries. *McNamara et al.* [2008] analyzed 30 days of $foF2$ obtained during the COPEX campaign and reported fairly good agreement between Boa Vista and Campo Grande during the evening hours. However, after 04:00 UT (post-midnight hours) they observed from the mean variations of $foF2$ that the collapse in the peak electron density occurs later in Campo Grande than in Boa Vista. As evidenced mainly from VHF data, this fact may explain in part the reason for the scintillations over Campo Grande to cease later than over Boa Vista. Other aspect which may help to understand the reason for the scintillations at GPS L-band and VHF frequencies to be more intense in Campo Grande than over the northern conjugate site of Boa Vista is presented in Fig. 4. In this figure mass plots of vertical drifts (V_z) calculated from the time rate of change of the F -layer true heights [$d(h'F)/dt$] for all days of the COPEX campaign is depicted for the three stations [see *Abdu et al.*, 2009 for more details]. The validity of the present method to determine the vertical drift of the evening equatorial ionosphere, in comparison with the measurement by other techniques, has been well documented in the literature [see for example, *Bertoni et al.*, 2006; *Abdu et al.*, 2006]. The vertical drift velocities calculated at each station are plotted versus UT and the time interval showed in the figure emphasizes the evening pre-reversal enhancement (PRE) in V_z . The solid curves in the plots denote mean V_z . We call the attention in this figure to the asymmetry in the PRE amplitude between the two conjugate sites, where the amplitude of the PRE over Campo Grande is larger (in $\sim 6 \text{ ms}^{-1}$) than over Boa Vista. According to *Abdu et al.* [2009] such asymmetry in the PRE amplitude over the conjugate sites is due to the

presence of a transequatorial neutral wind blowing northward. A large vertical drift over Campo Grande is displacing the ionosphere at F -layer heights to comparatively high altitudes and, probably, it is modifying the local ionosphere in such a way that create more conditions favorable to the triggering of secondary instability process. In addition, if plasma is moved upward to heights of decreased chemical losses, it contributes to an enhancement of electron density deviation of the irregularity and, consequently, may increase the strength of scintillations.

With the availability of simultaneous data of amplitude scintillation index (S_4), an attempt is made to compare the characteristics of the scintillations registered from the collocated GPS and VHF receivers at the COPEX sites. The results shown in Figs. 2 and 3 present high degree of correspondence in terms of morphological features of the scintillation pattern detected by the two instruments. A careful observation of the scintillation activity among the two conjugate stations and from the two different techniques shows nearly symmetrical features in the latitudinal extension of the scintillations during the first evening hours. Thus it reveals the coexistence of kilometer and hundred-meter scale irregularities into the underlying depletion structure. Other noticeable aspect seems to be related to the intensity of the scintillations. It is clearly seen from Figs. 2 and 3 that scintillations at VHF frequency is more intense than that at GPS L1 frequency. While between 23:00-02:00 UT the scintillation index S_4 at VHF is mostly within 0.7-1.1, the magnitude of the S_4 index at GPS L-band frequency is ranging from 0.3 to 0.7. It can also be seen from Figs. 2 and 3 that the hundred-meter scale structures responsible for the scintillations at GPS L1 frequency appear to decay faster than the kilometer scale structures that provoke scintillations at VHF. Thus, while the kilometer scale structures are still visible after 04:00 UT (post-midnight hours), the smaller scale structures causing the L-

band amplitude scintillations are practically absent. Again we draw the attention to the fact that, at the VHF frequencies, the importance of the background electron density seems to be comparatively lower than at the high L-band frequencies. This is clearly noted by comparing the scintillation activity detected close to the dip equator by the GPS receiver at Cachimbo, and that from the VHF receiver at Alta Floresta. While the magnitude of the S_4 index from the GPS L-band scintillations at Cachimbo rarely exceeds 0.4, the VHF scintillations at Alta Floresta are consistently higher and may assume saturated values of S_4 index. Moreover, the difference in the scintillation intensity between the magnetic conjugate points and the dip equator are more drastic for the GPS L1 frequency than for the VHF frequency, which also indicates the relative importance of the background electron density in causing the amplitude fluctuations at L-band.

The S_4 level that is above the noise and multipath effects is other important point to be commented from the comparison of the scintillations registered by the GPS and VHF receivers. The noise level of a receiver is critical to how it calculates S_4 and this includes several factors: The receiver's thermal noise, the antenna front to back gain ratios, the preamplification in the antenna, the length of the cable connecting the antenna to the receiver, the loss in the cables, and other concerns related to the receiver design such as the bandwidth of the tracking loop, the type of the control system (whether it is phase-locked-loop or frequency-locked-loop), and in the case of analog to digital (A/D) conversion the receiver needs the use of an automatic gain control (AGC) circuit to compensate for variations in RF signals strength (Paul M. Kintner, personal communication, 2008). The multipath effect is probably the most critical and difficult to quantify because it varies over a wide range depending on satellite position, obstructions such as buildings, trees, hills, and the surrounding terrain. Multipath occurs when both direct and reflected signals reach the

antenna causing signal variations on short time scales. Noise and multipath effects in general produce very weak scintillations. For the GPS receivers installed at the COPEX sites a S_4 level above 0.2 can be considered to overcome the noise and multipath effects. However, for the VHF receivers the scintillation intensity showed in Fig. 3 revealed, for all stations, a background blue contour during the time of no scintillation occurrence which suggests that the S_4 level of noise and multipath effect is between 0.18 and 0.36. We analyzed the VHF scintillation data and we found that a S_4 threshold of 0.25 can be considered, for all practical purposes, to be above the noise of level and multipath. These threshold levels of 0.2 for the GPS scintillation data and 0.25 for the VHF scintillation data have been used in the zonal drift estimations presented in the next section.

At VHF frequencies the occurrence of scintillations may be due to two types of irregularities, the EPB irregularities and the Bottom Side Sinusoidal (BSS) irregularities. While the former maximizes during post-sunset hours and can extend up to the topside F -region, the BSS irregularities according to *Valladares et al.* [1983] are observed mainly during post-midnight hours in a narrow altitude range about the bottomside F -region. Other difference among the two types of irregularities is related to their horizontal expansion. The BSS irregularities are in general confined to the equatorial belt of $\pm 12^\circ$ magnetic latitude and may extend up to 7500 km in the east-west direction [*Valladares et al.*, 1983], whereas the EPB irregularities extend to approximately $\pm 20^\circ$ from the dip equator and from tens to hundreds of kilometers in the east-west direction [*Schunk and Demars*, 2003]. Fortunately, from the amplitude scintillation pattern signatures, recorded by the VHF receivers, it is possible to differentiate most of the time the fluctuations caused by each type of irregularity. The scintillations due to EPBs in general present an abrupt onset and descent

with high magnitude of S_4 during post-sunset and pre-midnight hours. On the other hand, the scintillations due to BSS irregularities show a continuous patch that exists for comparative several hours (more than 6h) around post-midnight with moderate to high intensity, and with a quite slow conclusion of the scintillation event [Basu *et al.*, 1986]. The L-band frequencies have the advantage to be ‘invisible’ to the BSS irregularities and, thereby, the GPS scintillation records can be used to identify the similar plasma bubble structures sampled simultaneously by the VHF receiver. Different signatures of these irregularities can also be found from simultaneous observations with ionospheric sounders. For example, EPB irregularities manifest in the form of range type spread- F on ionograms, whereas BSS irregularities cause frequency type spread- F [Rao *et al.*, 2006]. The association of VHF scintillations with spread- F on ionograms and the symmetry/asymmetry characteristics of BSS irregularities during the COPEX campaign are not part of the scope of the present study, but deserve further investigation in a future work.

In terms of the time onset of the scintillations we have noticed from the VHF data that it may occur around 5-10 min earlier in Alta Floresta than at the conjugate stations of Boa Vista and Campo Grande. This time delay in the onset of the scintillations for the conjugate stations is due to the time required for the large scale bubbles, generated at the dip equator, to reach the apex height which maps along the magnetic field line to F -region heights over off-equatorial latitudes. Thus, a day-to-day variability in the time onset of the scintillations can be expected to occur as result of the daily variations in the polarization electric fields causing the vertical movement of the equatorial irregularities. A difference in the time onset of the scintillations compared from the GPS and VHF data have been found to vary mostly between 10-20 minutes at the conjugate sites. It is observed that the onset of the scintillations appears firstly at VHF. A frequency dependence on the onset of

scintillations at VHF and L-band frequencies are known to be very small [Franke and Liu, 1984], thus such difference can be probably due to geometrical factors, for which scintillations depends upon the position of the receiver relative to the irregularities in the ionosphere.

3.2 VHF and GPS Zonal Irregularity Drift Estimations

The zonal irregularity drift velocities concerned in this report are based on 11 geomagnetically quiet nights ($K_p < 3$) of simultaneous VHF and GPS scintillation-based spaced-antenna measurements. Only those amplitude scintillation envelopes having a similarly distinguishing structure at both VHF and GPS L-band data are considered in the zonal drift estimations. The top panels in Fig. 5 show the mean vertical drift velocity (V_Z) calculated from 4 MHz ionospheric true height data (for the 11 selected nights) and used to correct the contribution due to the vertical movement in the zonal drift estimations over Boa Vista (left panels) and Campo Grande (right panels). The middle and bottom panels show the mean zonal drift velocity of the scintillation pattern (V_{scint}) on the receiver plane and the mean zonal irregularity drift (V_{ion}) at IPP calculated, respectively, for the GPS L-band and VHF frequencies. It is seen from Fig. 5 that during the hours of the pre-reversal enhancement no drifts were calculated from the scintillation data. During this time period the scintillations are weak and the cross-correlation index (c_i) tend to be small due to the difference of the signal to noise ratio detected at the two antennas. After 23:00 UT the first zonal drifts are estimated and until about 01:00 UT it is found the largest contributions of V_Z in the scintillation pattern velocities (V_{scint}). In the station of Boa Vista during this time interval the largest difference between V_{scint} and V_{ion} observed from GPS calculations is 21 ms^{-1} and from VHF data is 39 ms^{-1} . For the northern conjugate station of Campo Grande

they are 26.5 ms^{-1} and 38.9 ms^{-1} , respectively, for the GPS and VHF calculations. The overall magnitude of the zonal irregularity drift velocities (V_{ion}) at Boa Vista for the GPS and VHF frequencies are, respectively, 4.3 ms^{-1} and 6.3 ms^{-1} larger than the zonal scintillation pattern velocity (V_{scint}). Whereas at the conjugate site of Campo Grande they are 4.8 ms^{-1} and 3.2 ms^{-1} , respectively, for the GPS and VHF zonal drift estimations.

Figure 6 presents a comparison of the averaged (30 min bins) zonal drift velocities estimated between the magnetic conjugate sites of Boa Vista and Campo Grande. It is observed from this figure that for both GPS (top panel) and VHF (bottom panel) measurements, the differences in the zonal drift velocities estimated at the magnetic conjugate sites are mostly within the standard deviation bars. In the case of GPS measurements it is noticed from the top panel of Fig. 6 that the Fresnel-scale (hundred meters) irregularity structures at Boa Vista and Campo Grande are drifting eastward with comparable velocities. The average GPS velocity estimated over Campo Grande is $\sim 6.5\%$ larger than over Boa Vista. In the case of VHF measurements (bottom panel), even though the σ bars overlaps at most of the time, it is possible to see that the averaged velocities are somewhat larger over the southern conjugate station of Campo Grande than in Boa Vista. It is found a nighttime average velocity $\sim 12\%$ larger in Campo Grande than over Boa Vista, whereas before 03:00 UT such differences may assume values of about 18%. One plausible explanation to this could be attributed to the differences in the magnitude of the total magnetic field intensity (B). It is known from published results that the zonal drifts of the well-developed irregularities can be considered to be equivalent to the ambient zonal plasma drift velocities [Terra *et al.*, 2004; Arruda *et al.*, 2006; Sobral *et al.*, 2009]. Thus, the irregularity drifts estimated in this report can be used as tracers of the ambient plasma. According to Haerendel *et al.* [1992], the resultant zonal velocity (V_s) of the plasma at F -

region heights equals to $-E_q/B$, where E_q denotes the vertical electric field at any given geomagnetic (dipole) latitude and B is the intensity of the total magnetic field, in which both are not invariant along the magnetic flux tubes. Recently, *Sobral et al.* [2009] showed from theoretical model that the zonal velocities of the ambient plasma using IGRF magnetic field values (at 250 km height) are ~24% larger over Campo Grande than those calculated over Boa Vista. The conjugate site of Campo Grande is close to the South Atlantic Magnetic Anomaly region (SAMA) where the intensity of B is lower than that at the northern conjugate point over Boa Vista. For example, according to the IGRF model the total magnetic field intensity at 350 km over Campo Grande (20,000 nT) is ~20% lower than over Boa Vista (25,150 nT). Thus, as result of the low magnetic field intensity, a large zonal plasma drift may exist over the South Atlantic hemisphere and, consequently, a comparative larger irregularity zonal velocity could be expected at the southern conjugate station of Campo Grande.

A comparison of the zonal irregularity drift velocities derived from GPS and VHF observations at each conjugate site is showed in Fig. 7. The estimated zonal irregularity drift velocities (V_{ion}) during the 11 nights are averaged for each 30 min time bins and plotted as function of universal time. The vertical bars indicate the standard deviations (σ) of the velocities. It is seen from this figure that the differences in the zonal drift velocities at Boa Vista estimated from GPS and VHF data (top panel) are mostly within the deviation bars and the magnitude of the velocities vary between ~100 and 185 ms^{-1} . The average zonal velocity estimated from VHF technique is ~4.75% larger than the average GPS velocity. Thereby, over Boa Vista the differences in the zonal velocities are not significant from the two techniques. Otherwise, in the southern conjugate station of Campo Grande

(bottom panel), even though the σ bars from both techniques overlaps most of the times, it is clear from this figure that before 02:00 UT the average velocities estimated from VHF data are larger than the GPS zonal drift estimations. While at Campo Grande a maximum magnitude of $\sim 185 \text{ ms}^{-1}$ is computed from GPS measurements at around 02:00 UT, in the case of VHF a maximum of $\sim 225 \text{ ms}^{-1}$ is observed around the same time. The average nighttime zonal drift velocity estimated from VHF technique is $\sim 10\%$ larger than the average GPS drift velocity, however, before 03:00 UT the average VHF velocities may attain values of $\sim 19\%$ larger than the GPS estimated velocities. From the comparison of the velocities estimated at the two frequencies it is also found that the zonal drifts show a tendency to increase slowly until their peak value between about 01:00-02:00 UT (before local midnight). After that the velocities start to abate until their minimum magnitudes around 04:00-05:00 UT when the large variations due to the electric fields (that cause large vertical drifts) become relatively small, which is consistent with the results reported previously by *Muella et al.* [2008b] and *Sobral et al.* [2009]. The discussions on the differences of the zonal drift velocities attributed to the possible effects of low magnetic field intensity at latitudes of Campo Grande are based only in the analysis of the average magnitude of the estimated zonal velocities. However, as reported from previous theoretical and experimental studies [e.g. *Haerendel et al.*, 1992; *Arruda et al.*, 2006; *Sobral et al.*, 2009] the lower local total magnetic field intensity will result in larger plasma and irregularity zonal drift velocities.

By comparing the results from L-band and VHF frequencies in terms of the scale size of the scintillation-producing irregularity density structures, the results for the magnetic conjugate stations suggest that the hundred meters and the kilometer scale irregularities can be considered drifting eastward at comparable velocities. Whether at Boa

Vista the VHF and GPS drift velocities are fitting very well, in the conjugate station of Campo Grande one might suggest that the kilometer scale irregularities inside the bubbles (causing VHF scintillations) seem to be drifting slightly faster than the hundred meter structures. Any difference in the zonal drift velocities estimate from GPS and VHF measurements could be associated to the fact that, in the case of GPS, the orbiting satellites are puncturing different irregularity structures in the sky above the station, while the geostationary satellite is always puncturing the ionosphere in a same point. Consequently, this geometrical factor might be contributing for discrepancies in the magnitude of the velocities when comparing both techniques. However, could any difference in the height distribution of the irregularities (with different scale-sizes) probed by each technique explain the differences observed at both conjugate sites from the simultaneous GPS/VHF estimated zonal drift velocities?

It is noticed from Figs. 4 and 5 larger vertical drifts over Campo Grande than over Boa Vista, which is probably contributing to the development of irregularities at comparative higher altitudes over the northern conjugate station. Thereby, if during the upwelling plasma the kilometer scale irregularities inside the bubbles are located in a more wide altitude range above the F -peak, it is possible that an altitude gradient (shear) could be contributing for their velocities to be higher than the velocities of the Fresnel-scale irregularities causing GPS scintillations. Therefore, this effect could explain the reason for the magnitude of the averaged VHF estimated zonal velocities in Campo Grande (bottom panel of Fig. 7) to be larger than the GPS estimated velocities. For example, *de Paula et al.* [2002] compared GPS and airglow measurements and showed that the smaller-scale irregularities can drift with zonal velocities larger than the large-scale plasma bubble structures. However, we point out that such differences are expected once that the airglow

inferred velocities by *de Paula et al.* [2002] are restricted to ~ 250 km, whereas the small-scale irregularities tend to be located in a more narrow altitude range about the F -peak where the electron density is high and steep density gradients exist. Therefore, GPS estimated drift velocities being larger than the airglow inferred drift velocities indicate the presence of a positive velocity shear with height [*Sobral et al.*, 2009], rather than a difference associated solely to the scale size structures.

In terms of errors in the zonal drift calculations one must consider the experimental errors. Assuming a drift velocity (V_{scint}) of 200 ms^{-1} the error will be 4% and 2%, respectively, for the GPS (50 Hz) and VHF (100 Hz) technique. The errors due to the difference between the apparent and true velocities (mainly before 21:00 UT) can be considered to be $< 10 \text{ ms}^{-1}$ for GPS [*Kil et al.*, 2000] and $< 20 \text{ ms}^{-1}$ for VHF (according to estimations not shown here). Other source of error may come from inaccuracies in the scaled ionospheric true height used to calculate vertical drift velocity contribution on Eqs. (1) and (2). According to *Muella et al.* [2008a] and *Fagundes et al.* [2008] digital ionosonde data ensures accuracies of about 1 km in scaling $h'F$, which result in an estimated error of about $\pm 7 \text{ ms}^{-1}$ in the effective vertical drift (V_z). Our results also rely on data obtained from IGRF model, and it is crucial to have in mind that the outputs of the model are assumed initially to be correct. Thus, uncertainties arising from inaccuracies in the IGRF model are not provided. These factors are found in both Eqs. (1) and (2) for VHF and GPS zonal drift estimations, respectively. However, for GPS drifts uncertainties may also be arising from GPS ephemeris (satellite velocity and position) error and on the assumed mean scattering height (h_{ion}). Satellite ephemeris bias can be considered a minor effect, since we used post-processed precise ephemerides and data between the spaced receivers, which minimizes error due to its high correlation over baselines. Regarding the

mean scattering height the well-accepted level of 350 km relate the location of the scintillation-causing irregularities to the height of maximum electron density. Although assumed, this mean scattering height is a good approximation since we used averaging over the scintillating GPS satellites [Kil *et al.*, 2000; de Paula *et al.*, 2002; Ledvina *et al.*, 2004] and observed nighttime mean values of $F2$ peak height ($hmF2$) parameter scaled from ionograms. The use of $hmF2$ is valid since the maximum contribution to the observed amplitude scintillation is from irregularities near the peak of the F region. In an average sense, the estimate of the zonal velocity with the mean scattering height of 350 km and the estimate with either 300 and 400 km produced a maximum error of 4 ms^{-1} (not shown here), which is also in agreement with the residual error calculations reported previously by Ledvina *et al.* [2004]. Hence, the factors mentioned above can be considered the main causes for discrepancies between the conjugate stations in the zonal drift velocities estimations for VHF and GPS techniques.

4. Remarks and Conclusions

This report concerns the results of magnetic conjugate point observations of kilometer and hundred meter scale irregularity structures monitored, respectively, by VHF and GPS ground-based instruments. The measurements of amplitude scintillations at VHF and GPS L-band frequencies were obtained from examining data acquired during the COPEX campaign and carried out from October to December 2002. The zonal drift velocities of the different irregularity scale sizes during the campaign period were estimated over 11 geomagnetically quiet nights of simultaneous VHF and GPS spaced antenna system observations. The main results of the present work are summarized as follows.

VHF and L-band scintillations measurements at the COPEX sites reveal the coexistence of kilometer and hundred-meter scale irregularity structures into the underlying plasma depletion. However, the kilometer scale structures causing VHF scintillations tend to decay slower than the hundred meter scale structures, which demonstrate the relative importance of background electron density in causing L-band scintillations. It is noticed from the results that scintillation activity is more intense at the conjugate sites of Boa Vista and Campo Grande than over the equatorial stations, owing to the increased background electron density and sharp electron density gradients that exist at latitudes adjacent to the crests of the equatorial ionization anomaly. Moreover, the scintillations seem to be more intense over Campo Grande than over Boa Vista, which can be attributed to the combination effects of large post-sunset vertical plasma drift and delayed collapse in peak electron density (over Campo Grande). For future work, the present observations suggest that it would be interesting to analyze some important aspects of the thermosphere-ionosphere system, such as the role on equatorial scintillation activity, played by the $\mathbf{E} \times \mathbf{B}$ drift velocities, the $F2$ -peak density gradients and the thermospheric neutral winds.

The daily observations of GPS and VHF measurements reveal asymmetrical features in the intensity and latitudinal distribution of the scintillations. Thus, the day-to-day variability in the ambient ionization and in the electron density gradients could be a possible cause for the corresponding asymmetries observed over the magnetic conjugate sites. This implies that whether intense horizontal $F2$ -peak density gradients exist between the dip equator and the EIA crests, secondary instability process that create conditions favorable for the generation of smaller scale plasma irregularities may be set up at the walls of a well-developed large scale bubble that extend/expand along the magnetic field lines.

The VHF estimated zonal irregularity drift velocities are on average ~4.75% and ~10% larger than the GPS velocities, respectively, for Boa Vista and Campo Grande. Over Campo Grande and before 03:00 UT the average VHF velocities may attain values of ~19% larger than the GPS estimated velocities. However, the differences in the zonal drift velocities are mostly within the standard deviation bars. Whether during the upwelling plasma the kilometer scale irregularities (inside the bubbles) causing VHF scintillations are located in a more wide altitude range above the F -peak, and the smaller scale structures are in a more narrow altitude range about the F -peak (where the electron density is high and steep density gradient is present), it is possible that an altitude gradient (shear) could be contributing for the VHF velocities to be higher than the GPS estimated velocities. There should be also a contribution due to geometrical factors on the differences seen from both techniques. In turn, the comparative large vertical plasma drift velocity over Campo Grande is probably contributing for a higher vertical shear of the plasma flow over this station.

On average the GPS zonal drift velocities over Campo Grande is ~6.5% larger than over the magnetic conjugation site of Boa Vista, whereas for the VHF estimations the irregularity drift velocities over the southern conjugate station of Campo Grande is ~12% larger than over Boa Vista. Before 03:00 UT the VHF velocities over Campo Grande may assume values of about 18% higher than over Boa Vista. Based on previous modeling results [e.g. *Sobral et al.*, 2009] we may conclude that the larger eastward drift velocities observed over Campo Grande can be attributed to the comparative weaker total magnetic field intensity (considering a dipole configuration of the magnetic field) that exists over the South Atlantic hemisphere. In a future work, we hope that the present report can stimulate further experimental and theoretical studies about the effects of the geomagnetic field

strength that drive the overall electrodynamics and its relation to the variation of irregularity occurrence and zonal drift velocities.

Acknowledgments

The authors thank the Brazilian Air Force for their logistical support and facilities provided for the carrying out of the COPEX campaign. The authors also thank Drs. Robert Livingston (SCION Associates), Robert Sheehan and Santimay Basu for the valuable comments on the methodologies used in the present work. Marcio Muella acknowledges the Post-Doctoral fellowship provided by the Fundação de Amparo à Pesquisa do Estado de São Paulo (FAPESP) under Project No. 2008/04892-5. This research was also partially supported by the Coordenação de Aperfeiçoamento de Pessoal de Nível Superior (CAPES) under process No. BEX3367/05-3.

References

Abdu, M.A., 1997. Major phenomena of the equatorial ionosphere-thermosphere system under disturbed conditions. *J. Atmos. Solar-Terr. Phys.* 13, 1505-1519.

Abdu, M.A., Batista, I.S., Reinisch, B.W., Sobral, J.H.A., Carrasco, A.J., 2006. Equatorial F region evening vertical drift during southern winter months: A comparison of observational data with IRI descriptions. *Adv. Space Res.* 37, 1007– 1017.

Abdu, M. A., Batista, I. S., Reinisch, B. W., Souza, J. R., Sobral, J. H. A., Bertoni, F., Pedersen, T. R., Medeiros, A. F., Schuch, N. J., de Paula, E. R., Groves, K. M., 2009. Conjugate Point Equatorial Experiment (COPEX) Campaign in Brazil: Electrodynamics

highlights on spread F development conditions and day-to-day variability. *J. Geophys. Res.* 114, A04308, doi: 10.1029/2008JA013749.

Arruda, D.C.S., Sobral, J.H.A., Abdu, M.A., Castilho, V.M., Takahashi, H., Medeiros, A.F., Buriti, R.A., 2006. Theoretical and experimental zonal drift velocities of the ionospheric plasma bubbles over the Brazilian region. *Adv. Space Res.* 38, 2610-2614.

Basu, S., Basu, S., Aarons, J., McClure, J. P., Cousins, M. D., 1978. On the coexistence of kilometer and meter-scale irregularities in nighttime F region. *J. Geophys. Res.* 83, 4219-4226.

Basu, S., Basu, S., Valladares, C. E., DasGupta, A., Whitney, H. E., 1986. Scintillations associated with bottomside sinusoidal irregularities in the equatorial F-region. *J. Geophys. Res.* 91, 270-276.

Batista, I. S., Abdu, M. A., Carrasco, A. J., Reinisch, B. W., de Paula, E. R., Schuch, N. J., Bertoni, F., 2008. Equatorial spread F and sporadic E-layer connections during the Brazilian Conjugate Point Equatorial Experiment (COPEX). *J. Atmos. Solar-Terr. Phys.* 70, 1133-1143.

Beach, T. L., Kintner, P. M., 1999. Simultaneous Global Positioning System observations of equatorial scintillations and total electron content fluctuations. *J. Geophys. Res.* 104, 22,553-22,565.

Beach, T. L., Kintner, P. M., 2001. Development and use of a GPS ionospheric scintillation monitor. *IEEE Transac. Geosci. Rem. Sensing* 39, 918-928.

Bertoni, F., Batista, I.S., Abdu, M.A., Reinisch, B.W., Kherani, E.A., 2006. A comparison of ionospheric vertical drift velocities measured by Digisonde and Incoherent Scatter Radar at the magnetic equator. *J. Atmos. Solar-Terr. Phys.* 68, 669-678.

de La Beaujardière, O; CNOFS Science Definition Team, 2004. C/NOFS: a mission to forecast scintillations. *J. Atmos. Solar-Terr. Phys.* 66, 1573-1591.

de Paula, E. R., Kantor, I. J., Sobral, J. H. A., Takahashi, H., Santana, D. C., Gobbi, D., Medeiros, A. F., Limiro, L. A. T., Kil, H., Kintner, P. M., Taylor, M. J., 2002. Ionospheric irregularity zonal velocities over Cachoeira Paulista. *J. Atmos. Solar-Terr. Phys.* 64, 1511-1516.

de Paula, E. R., Kherani, E. A., Abdu, M. A., Batista, I. S., Sobral, J. H. A., Kantor, I. J., Takahashi, H., de Rezende, L. F. C., Muella, M. T. A. H., Rodrigues, F. S., Kintner, P. M., Ledvina, B. M., Mitchell, C. N., Groves, K. M., 2007. Characteristics of the ionospheric F-region plasma irregularities over Brazilian longitudinal sector. *Indian J. Radio Space Phys.* 36, 268-277.

Fagundes, P.R., Muella, M.T.A.H., Bittencourt, J.A., et al., 2008. Nighttime ionosphere-thermosphere coupling during geomagnetic storms. *Adv. Space Res.* 41, 539-547.

Franke, S. J., Liu, C. H., 1984. Interpretation and modeling of quasiperiodic diffraction patterns observed in equatorial VHF scintillation due to plasma bubbles. *J. Geophys. Res.* 89, 891-902.

Haerendel, G. E., 1973. Theory of equatorial spread F. Report, Maxplanck-Institut fur Extraterre. Phys. Garching, Germany.

Haerendel, G. E., Eccles, J. V., Çakir, S., 1992. Theory of modeling the equatorial evening ionosphere and the origin of the shear in the horizontal plasma flow. *J. Geophys. Res.* 97, 1209-1223.

Kil, H., Kintner, P. M., de Paula, E. R., Kantor, I. J., 2000. Global Positioning System measurements of the ionospheric zonal apparent velocity at Cachoeira Paulista in Brazil. *J. Geophys. Res.* 105, 5317-5327.

Kintner, P. M., Ledvina, B. M., de Paula, E. R., Kantor, I. J., 2004. Size, shape, orientation, speed, and duration of GPS equatorial anomaly scintillations. *Radio Sci.* 39, RS2012, doi:10.1029/2003RS002878.

Kintner, P. M., Ledvina, B. M., 2005. The ionosphere, radio navigation, and global navigation satellite systems. *Adv. Space Res.* 35, 788-811.

Ledvina, B. M., Kintner, P. M., de Paula, E. R., 2004. Understanding spaced-receiver zonal velocity estimation. *J. Geophys. Res.* 109, A10306, doi:10.1029/2004JA010489.

Makela, J. J., 2006. A review of imaging low-latitude ionospheric irregularity processes. *J. Atmos. Solar-Terr. Phys.* 68, 1441-1458.

Maruyama, T., 1988. A diagnostic model for equatorial spread-F: 1. Model description and application to electric-field and neutral wind effects. *J. Geophys. Res.* 93, 14611-14622.

McDougall, J., Abdu, M. A., Batista, I. S., 2009. Conjugate sporadic-E measurements. *J. Atmos. Solar-Terr. Phys.* 71, 1333-1339.

- McNamara, L. F., Retterer, J. M., Abdu, M. A., Batista, I. S., Reinisch, B. W., 2008. F2 peak parameters, drifts and spread F derived from digisonde ionograms for the COPEX campaign in Brazil. *J. Atmos. Solar-Terr. Phys.* 70, 1144-1158.
- Muella, M.T.A.H., Fagundes, P.R., Bittencourt, J.A., Sahai, Y., Lima, W.L.C., Becker-Guedes, F., Pillat, V.G., 2008a. Nighttime thermospheric meridional neutral winds inferred from ionospheric $h'F$ and $hpF2$ data. *Adv. Space Res.* 41, 599-610.
- Muella, M. T. A. H., de Paula, E. R., Kantor, I. J., Batista, I. S., Sobral, J. H. A., Abdu, M. A., Kintner, P. M., Groves, K. M., Smorigo, P. F., 2008b. GPS L-band scintillations and ionospheric irregularity zonal drifts inferred at equatorial and low-latitude regions. *J. Atmos. Solar-Terr. Phys.* 70, 1261-1272.
- Muella, M. T. A. H., de Paula, E. R., Kantor, I. J., Rezende, L. F. C., Smorigo, P. F., 2009. Occurrence and zonal drifts of small-scale ionospheric irregularities over an equatorial station during solar maximum – Magnetic quiet and disturbed conditions. *Adv. Space Res.* 43, 1957-1973.
- Muella, M.T.A.H., Kherani, E.A., de Paula, E.R., Cerruti, A.P., Kintner, P.M., Kantor, I.J., Mitchell, C.N., Batista, I.S., Abdu, M.A., 2010. Scintillation-producing Fresnel-scale irregularities associated with the regions of steepest TEC gradients adjacent to the equatorial ionization anomaly. *J. Geophys. Res.*, 115, A03301, doi:10.1029/2009JA014788.
- Muralikrishna, P., 2000. F-region electron density irregularities during the development of equatorial plasma bubbles. *Geof. Internacional* 39, 117-125.

Pi, X., Mannucci, A. J., Lindqwister, U. J., Ho, C. M., 1997. Monitoring of global ionospheric irregularities using the world-wide GPS network. *Geophys. Res. Lett.* 24, 2283-2286.

Rao, P.V.S.R., Krishna, S.G., Niranjana, K., Prasad, D.S.V.V.D., 2006. Study of spatial and temporal characteristics of L-band scintillations over the Indian low-latitude region and their possible effects on GPS navigation. *Ann. Geophys.* 24, 1567-1580.

Reinisch, B.W., Abdu, M.A., Batista, I.S., Sales, G.S., Khmyrov, G., Bulet, T.A., Chau, J., Rios, V., 2004. Multistation digisonde observations of equatorial spread *F* in South America. *Ann. Geophys.* 22, 3145-3153.

Sahai, Y., Bittencourt, J. A., Teixeira, N. R., Takahashi, H., 1981. Plasma irregularities in the tropical F-region detected by OI 7774 A and 6300 A nightglow. *J. Geophys. Res.* 86, 3496-3500.

Schunk, R.W., Demars, H.G., 2003. Effect of the equatorial plasma bubbles on the thermosphere. *J. Geophys. Res.* 108, 1245, doi: 10.1029/2002JA009690.

Sobral, J. H. A., Abdu, M. A., Pedersen, T. R., Castilho, V. M., Arruda, D. C. S., Muella, M. T. A. H., Batista, I. S., Mascarenhas, M., de Paula, E. R., Kintner, P. M., Kherani, E. A., Medeiros, A. F., Buriti, R. A., Takahashi, H., Schuch, N. J., Denardini, C. M., Zamlutti, C. J., Pimenta, A. A., Souza, J. R., Bertoni, F. C. P., 2009. Ionospheric zonal velocities at conjugate points over Brazil during the COPEX campaign: Experimental observations and theoretical validations. *J. Geophys. Res.* 114, A04309, doi:10.1029/2008JA013896.

Terra, P.M., Sobral, J.H.A, Abdu, M.A., Souza, J.R., Takahashi, H., 2004. Plasma bubble zonal velocity variations with solar activity in the Brazilian region. *Ann. Geophys.* 22, 3123-3128.

Valladares, C. E., Hanson, W. B., McClure, J. P., Cragin, B. L., 1983. Bottomside sinusoidal irregularities in the equatorial F-region. *J. Geophys. Res.* 88, 8025-8042.

Figure Captions

Figure 1. A map showing COPEX geometry and the localization of the observation sites: Cachimbo and the magnetic conjugate stations of Boa Vista and Campo Grande.

Figure 2. Contour plots for the GPS L-band amplitude scintillation activity (S_4 index) obtained at the three stations of the COPEX campaign (Boa Vista, Cachimbo and Campo Grande) throughout October-December 2002. The color scale bars indicate the S_4 index level. [After *Muella et al.* 2008b]

Figure 3. Contour plots for the VHF amplitude scintillation activity (S_4 index) obtained at three stations of the COPEX campaign (Boa Vista, Alta Floresta and Campo Grande) throughout October-December 2002.

Figure 4. Mass plotted vertical drift velocity (V_z) inferred over three COPEX sites (Boa Vista, Cachimbo and Campo Grande) during the entire campaign period. The solid curves denote mean vertical drift. [After *Abdu et al.* 2009]

Figure 5. Digisonde vertical drift velocity (top panels), GPS (middle panels) and VHF (bottom panels) zonal scintillation pattern velocity (scattered triangles) and irregularity zonal drift velocity (red asterisks) estimated for the conjugate sites of Boa Vista (left column) and Campo Grande (right column).

Figure 6. Comparison of the average zonal drift velocities estimated in the magnetic conjugate stations of Boa Vista (line with blanket squares) and Campo Grande (line with asterisks) from GPS (top panel) and VHF data (bottom panel).

Figure 7. Comparison of the average zonal drift velocities estimated from GPS (line with blanket squares) and VHF (line with asterisks) in the magnetic conjugate stations of Boa Vista (top panel) and Campo Grande (bottom panel).

Tables and Table Captions

Table 1. Azimuth and elevation of the signal paths as observed at three of the COPEX sites.

Stations	Channel 1-2 (west)		Channel 3-4 (east)	
	Azimuth	Elevation	Azimuth	Elevation
Boa Vista	266.6°	44.4°	93.6°	46.2°
Alta Floresta	279.9°	38.3°	75.5°	50.2°
Campo Grande	289.1°	34.0°	60.4°	46.9°

Table 2. Coordinates of the subionospheric points from signals of satellite FLEETSAT-8 to the receivers located at three of the COPEX sites.

Subionospheric coordinates		
Satellite-to-receiver signal path	Latitude (ϕ_{pp})	Longitude (λ_{pp})
Boa Vista	$\phi_{350} = 2.62^\circ \text{ N}$	$\lambda_{350} = 57.9^\circ \text{ W}$
Alta Floresta	$\phi_{620} = 8.65^\circ \text{ S}$	$\lambda_{620} = 51.9^\circ \text{ W}$
Campo Grande	$\phi_{350} = 19.13^\circ \text{ S}$	$\lambda_{350} = 52.2^\circ \text{ W}$

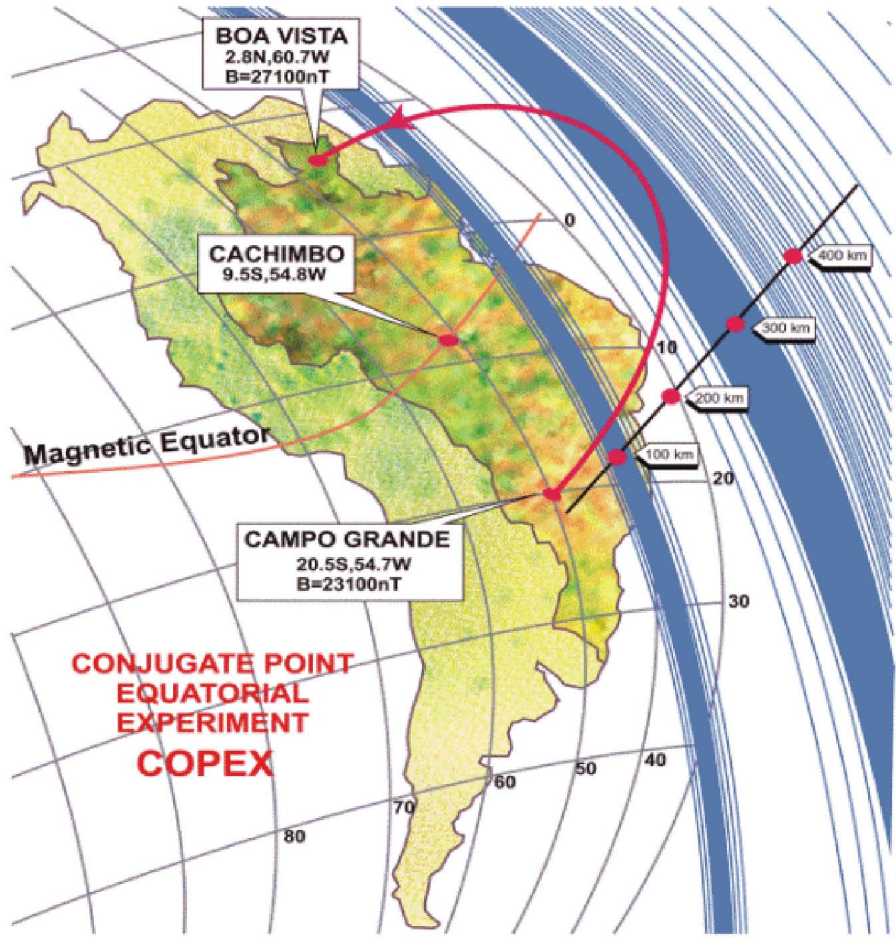
BOA VISTA
2.8N,60.7W
B=27100nT

CACHIMBO
9.5S,54.8W

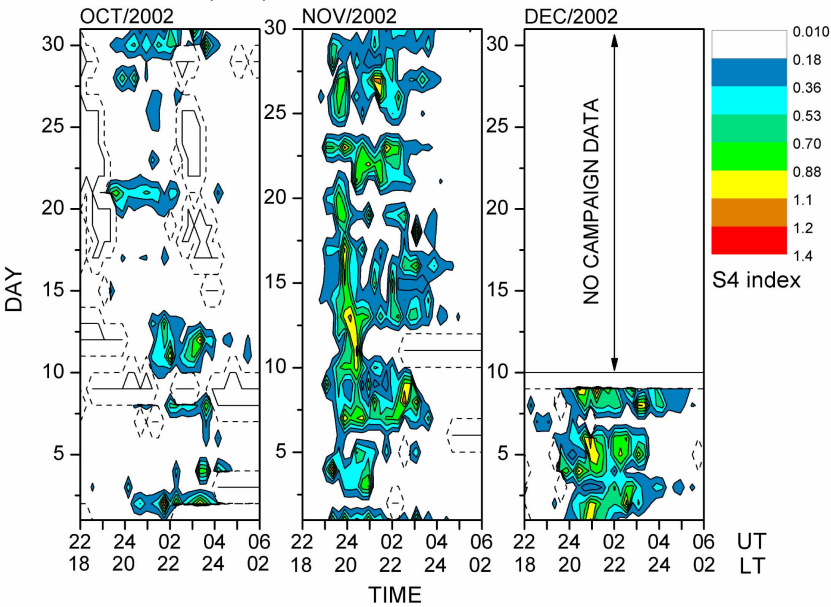
CAMPO GRANDE
20.5S,54.7W
B=23100nT

Magnetic Equator

**CONJUGATE POINT
EQUATORIAL
EXPERIMENT
COPEX**



BOA VISTA (GPS)



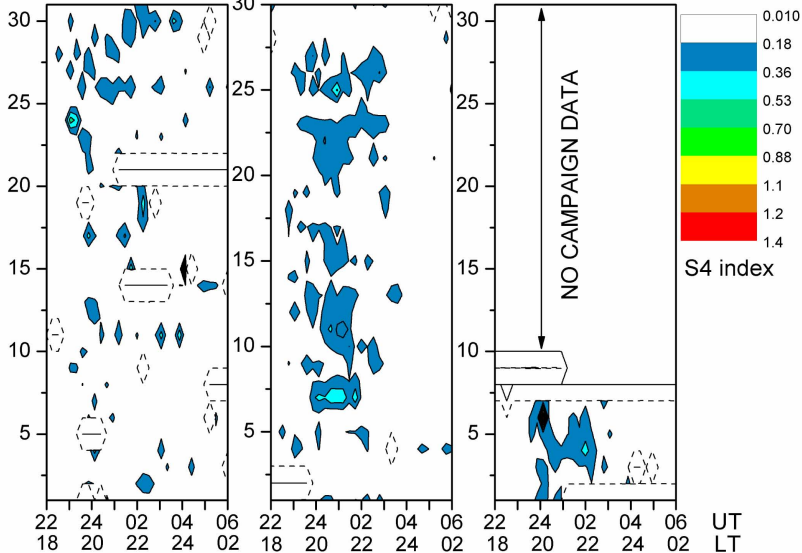
CACHIMBO (GPS)

OCT/2002

NOV/2002

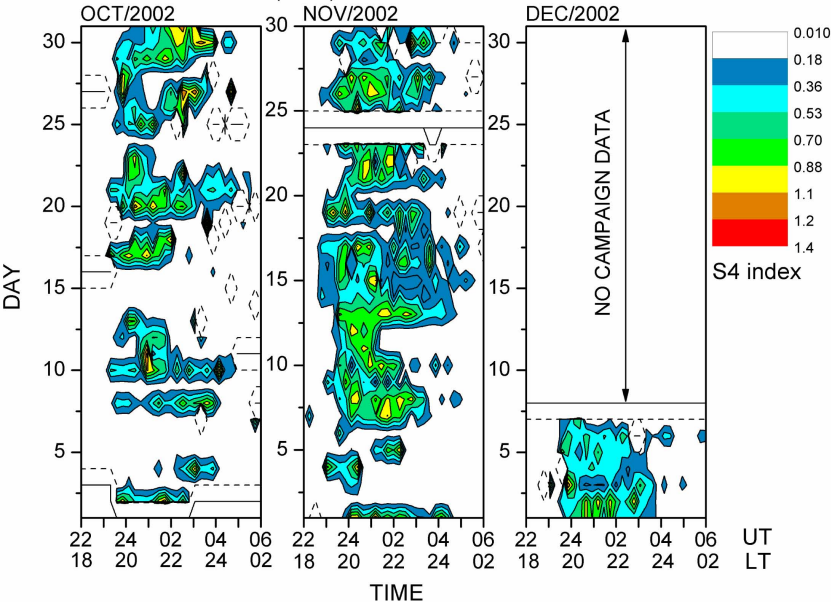
DEC/2002

DAY

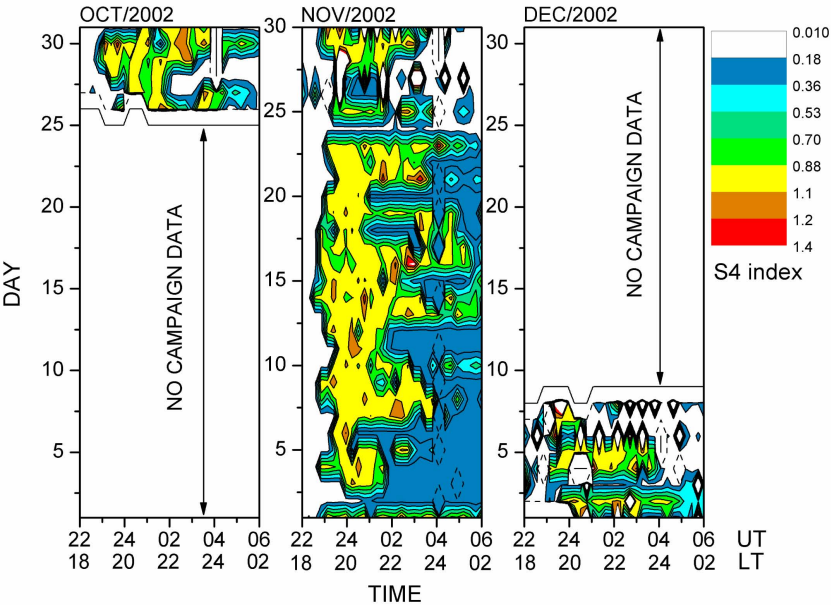


TIME

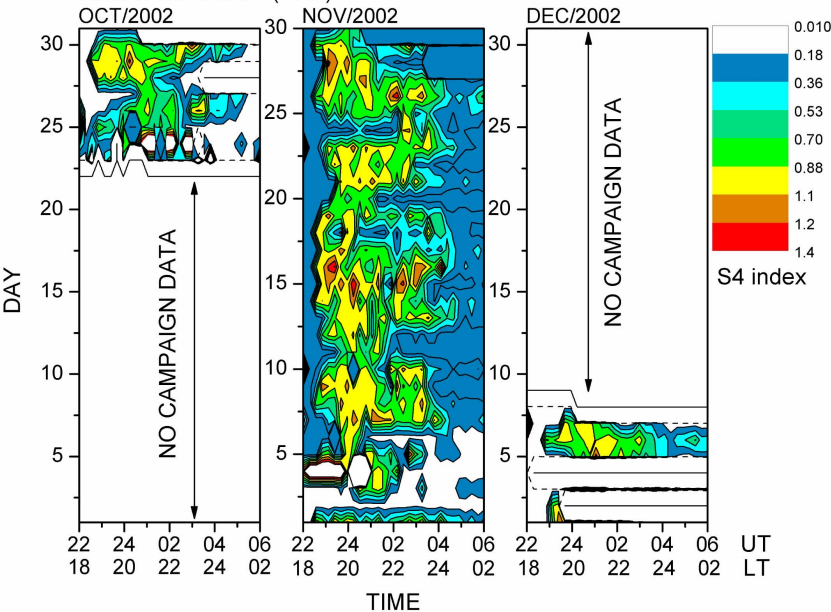
CAMPO GRANDE (GPS)



BOA VISTA (VHF)



ALTA FLORESTA (VHF)



CAMPO GRANDE (VHF)

